published in: *Materials Science and Engineering B* **159-160**, p. 44-47 (2009)
http://dx.doi.org/10.1016/j.mseb.2008.10.050

Improved homogeneity of microcrystalline absorber layer in thin-film silicon tandem solar cells

V. Smirnov *, C. Das, T. Melle, A. Lambertz, M. Hülsbeck, R. Carius, F. Finger

IEF-5 Photovoltaik, Forschungszentrum Jülich, D-52425 Jülich, Germany

Keywords:

Microcrystalline silicon
Solar cells
PECVD
Nucleation
Growth

Abstract

A study of the effects of microcrystalline silicon i-layer modification near p/i interface in tandem configuration silicon thin film solar cells is presented. The structural properties of the absorber layers were investigated by Raman spectroscopy at different stages of growth. The results indicate the possibility of improving both the nucleation process and the film homogeneity in the direction of growth, without specific re-optimization of the p-layer, transferred from a single-junction microcrystalline silicon cell. Structural modifications of the i-layer have been correlated with performance of tandem solar cells, leading to improvements in the bottom cell current J_{SC} (up to 11.4 mA/cm^2) and initial tandem-cell conversion efficiency (up to 11.3%).

1. Introduction

Microcrystalline silicon (μc-Si) has received significant attention as intrinsic thin film layer in bottom component of multijunction thin silicon film solar cells due to its enhanced response in longer wavelength part of the solar spectrum and higher stability against light induced degradation. Microcrystalline silicon is a mixed phase material containing columns or clusters of crystalline grains, disordered regions and voids [1], and its electronic and structural properties have been the subject of intensive research. The growth of μc-Si films prepared by PECVD is known to be substrate dependent [2-5]. In the early stages of growth its microstructure changes significantly with the deposition time [6] and an incubation layer is frequently observed. In the case of photovoltaic devices, deposited in a p–i–n sequence, the microcrystalline silicon active layer is deposited on to the p-layer, which therefore must provide nucleation centres for μc-Si i-layer growth [7]. In a single junction device, p-layer growth should be optimised directly on TCO. In the case of tandem configuration however, where the p-layer is grown on the n-layer of the top cell, the recipe for an optimal single junction cell can no longer be used, since the p-layer requirements are different in each case. Thus, the recipe may need to be re-optimized (particularly the p- and i-layer) when transferred into tandem configuration.

* Corresponding author.
E-mail address: v.smirnov@fz-juelich.de (V. Smirnov).

It has been shown that the performance of a solar cell, utilizing μc-Si as an absorber layer, is strongly dependent on crystalline volume fraction [8]. Additionally, structural homogeneity of the active layer in the direction of growth was suggested as a possible requirement for improved single junction solar cell performance [9]. A method for improving the i-layer homogeneity in microcrystalline silicon cells deposited in n–i–p sequence was suggested by utilizing a hydrogen dilution profiling method [10]. In that case, the i-layer is grown on the n-layer of the cell and the silane concentration ratio is modified over the total growth time.

Here, we present a study of the effects of microcrystalline silicon i-layer modification near p/i interface in a tandem solar cell configuration. The results from Raman spectroscopy are correlated with solar cell performance, and a relatively simple method to maintain a homogeneous i-layer growth with a desirable crystallinity, independently on p-layer nucleation properties, leading to an improved solar cell performance, is presented.

2. Experimental details

Silicon thin films were deposited by plasma enhanced chemical vapour deposition (PECVD) technique using either RF (13.56 MHz) or VHF (94.7 MHz) excitation for different intrinsic and extrinsic layers. In the deposition of microcrystalline silicon intrinsic layer a gas mixture of silane (SiH4) and hydrogen (H_2) was used. The intrinsic μc-Si layers were deposited using VHF excitation at a power density of

published in: *Materials Science and Engineering B* **159-160**, p. 44-47 (2009)
http://dx.doi.org/10.1016/j.mseb.2008.10.050

0.13 W/cm^2. The substrate temperature and chamber pressure for the deposition of i-layer was fixed at 180 °C and 1.5 mbar respectively. The silane concentration ratio SC = [SiH_4]/([SiH_4] + [H_2]) was kept at 5%. However, for several cells, the initial growth conditions were modified near the p/i interface by reduction of SC to 4% for up to 6 min. The details of i-layer modification are summarised in Table 1.

Table 1. Process gas parameters of microcrystalline silicon i-layer.

Cell number	Initial growth		Total growth	
	SC (%)	Thickness (nm)	SC (%)	Thickness (nm)
1	5	0	5	1500
2	4	70	5	1500
3	4	110	5	1500

The structure of the a-Si/μc-Si tandem solar cell is as following: glass/ZnO(texture-etched)/p–i(a-Si)–n/p–i(μc-Si)–n/ZnO–Ag. The deposition conditions of a-Si intrinsic layer, n-type and p-type layers remained unaltered while μc-Si i-layer properties were varied. The area of the individual devices is defined by the 1 cm^2 ZnO–Ag back contacts. The metal and TCO layers were deposited using thermal evaporation and RF sputtering, respectively.

The structural properties of the intrinsic μc-Si layer were probed using Raman spectroscopy, with excitation at 488 nm supplied by an Ar-ion laser. At this wavelength, the penetration depth in microcrystalline silicon is around 150–200 nm [9,11]. Raman measurements were performed directly on the solar cells, after the removal of n-layer by chemical etching with KOH solution. Additionally, craters with different depths were created by KOH etching to obtain information on the structural evolution in the direction of growth. This method can provide direct information about i-layer structural properties at different stages of growth and its relationship [12] with solar cell performance. The etched craters were measured by Veeco Dektak-6M surface profiler. A typical depth profile of a crater is shown in Fig. 1. The Raman setup is equipped with an optical system which enables the laser to be focused down to 10 μm and positioned on the sample with high spatial resolution. The ratio of integrated intensities of Gaussian peaks fitted to the Raman signal attributed to crystalline and amorphous regions, $I_{CRS} = I_c/(I_c + I_a)$ was used a semi-quantitative value of the crystalline volume fraction [1].

Solar cells were characterized at 25 °C by current–voltage (I–V) measurements under AM1.5 illumination from a solar simulator. The open-circuit voltage (V_{oc}), short-circuit current density (J_{sc}) and fill factor (FF) were used to calculate the conversion efficiency (η) of the solar cells. The spectral response of the solar cells was measured and the quantum efficiency (QE) in the range of 350–1000 nm calculated. The integrated current from the quantum efficiency curves under short-circuit conditions has been used to evaluate the short-circuit current (J_{sc}) from the component cells.

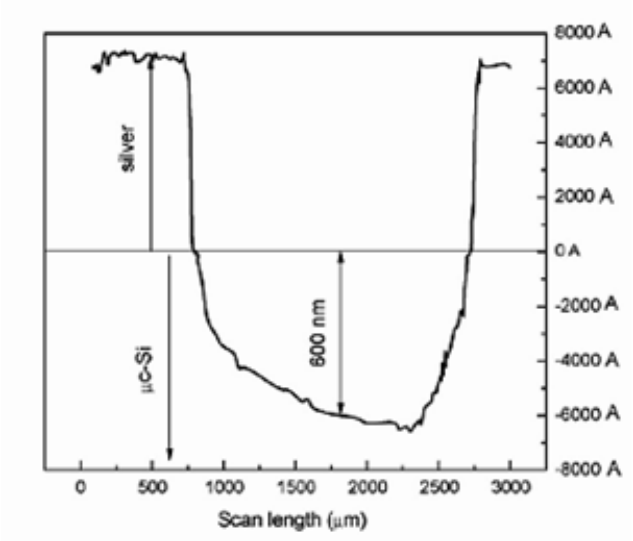

Fig. 1. A typical depth profile of a crater etched by a KOH solution. The etching was performed between two silver pads down to around 600 nm depth.

3. Results and discussion

Fig. 2 shows the Raman spectra for microcrystalline silicon i-layer craters, measured at different depths. The spectra are normalized to the highest peak intensities. The arrows indicate a microstructure evolution with etching depth, the calculated I_{CRS} values are quoted for the lowest and highest values. The Raman spectra of non-modified microcrystalline silicon i-layer (cell 1) shows a broad intensity profile at approximately 480 cm^{-1} (see Fig. 2a), associated with amorphous phase contribution. When the etching depth reaches a few tens of nm, the intensity of the 480 cm^{-1} peak is significantly reduced. In contrast, the i-layer Raman spectra of cells 2 and 3, grown with initial i-layer modification (see Fig. 2b and c, respectively), show an increased crystalline contribution.

Fig. 3 shows the calculated I_{CRS} for cells 1–3, measured at different crater depths in the i-layer of microcrystalline silicon bottom cell. Position "0 nm" corresponds to the position of the n-layer. It can be seen that cell 1, prepared without i-layer modification, shows a significant structural evolution, from a largely amorphous microstructure near the p–i interface to significantly crystalline, with I_{CRS} around 30%. This trend is largely consistent with previous reports on microcrystalline silicon growth without nucleation support from a substrate (for example on glass or amorphous silicon film) [4], [6] and [13]. The results of cell 1 suggest that the p-layer is not optimised in terms of nucleation properties for microcrystalline silicon i-layer growth. Improvement of the p-layer nucleation

published in: *Materials Science and Engineering B* **159-160**, p. 44-47 (2009)
http://dx.doi.org/10.1016/j.mseb.2008.10.050

properties in tandem solar cell configuration would involve a complicated procedure, since the p-layer must fulfil the requirements of a window and doped layer [7], and the pn contact between top and bottom cells must function as an effective recombination junction.

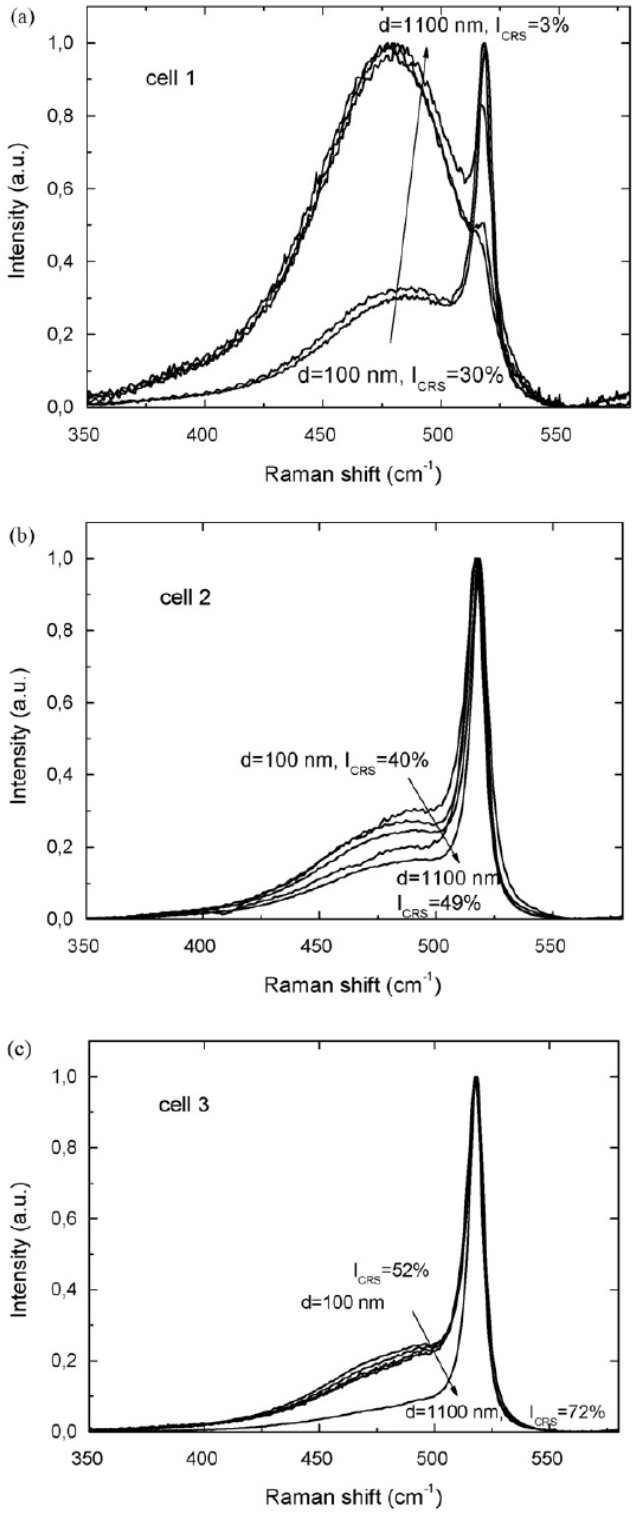

Fig. 2. Raman scattering spectra of microcrystalline silicon i-layer, measured at different etching depths (d). (a) cell 1, (b) cell 2 and (c) cell 3. The calculated I_{CRS} values are indicated for the lowest and highest values.

Instead of trying to improve the p-layer nucleation properties, cells 2 and 3 were deposited with i-layer conditions modified near the p/i interface. In the case of these two cells, the results of Raman measurements indicate higher crystallinity values during initial growth, in comparison with cell 1. A prolonged i-layer modification (up to 6 min for cell 3) results in increased crystallinity. Further increase in silane concentration (see Table 1, "total growth conditions") during film growth, reduces crystalline volume fraction in the i-layer, although it is still maintained at a relatively high level. The results suggest that modification of the i-layer initial growth provides improved nucleation [4, 7, 11] for continuous i-layer growth. Fig. 3 also demonstrates that the two-step i-layer modification method used here for cells 2 and 3 (see Table 1) is able to maintain a good homogeneity in the direction of growth.

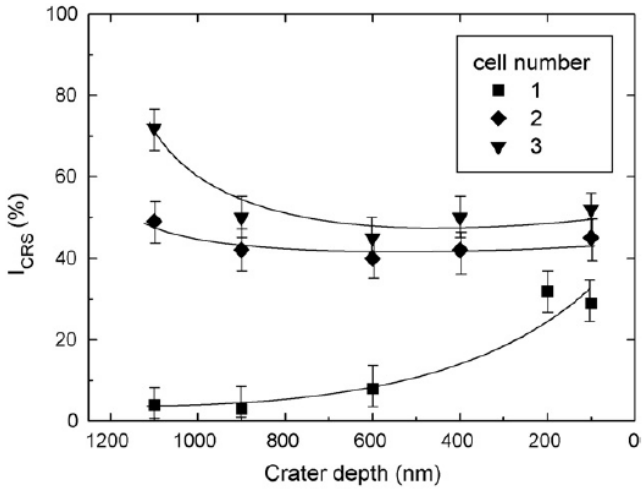

Fig. 3. Calculated I_{CRS}, measured at different stages of growth in the i-layer. The measurement error for crater depth values is less then 50 nm.

The performance of the cells is summarised in Table 2. It shows that the performance of tandem cell 1 is poor because the current density from the bottom cell is too low. It also shows a high V_{oc} value, that is consistent with a higher amorphous volume fraction in the i-layer material. This is supported by the structural data presented in Fig. 2 and Fig. 3. Such poor performance results from the non-optimised microcrystalline silicon i-layer growth, which may in turn arise from a non-optimized, in terms of nucleation properties, p-layer structure.

Modification of the initial i-layer growth results in an increase in the bottom cell current density, from 5 to 9.4 mA/cm^2 and 11.4 mA/cm^2 for cells 2 and 3, respectively. The overall solar cell parameters (V_{oc}, J_{sc} and FF) remain encouragingly high for cell 3, indicating that the p-layer is performing well in its functions as doped layer, window and recombination layer, while the

published in: *Materials Science and Engineering B* **159-160**, p. 44-47 (2009)
http://dx.doi.org/10.1016/j.mseb.2008.10.050

p-layer nucleation properties may be relaxed. A conversion efficiency of 11.3% has been achieved for cell 3.

Table 2. I–V parameters of tandem solar cells under AM1.5 illumination.

Cell number	V_{oc} (V)	FF	J_{sc} (mA/cm^2)		η (%)
			Top	Bottom	
1	1.47	0.77	11.7	5.0	5.7
2	1.42	0.77	11.0	9.4	10.3
3	1.41	0.73	11.0	11.4	11.3

It was previously shown that optimal microcrystalline silicon cell performance is achieved when the absorber layer is deposited close to the amorphous to microcrystalline transition region [8]. Fig. 3 indicates that in the case of cells 2 and 3, the microcrystalline silicon i-layer microstructure is maintained near I_{CRS} = 50% region over the probed depths. Our results indicate that a simple two-step modification of the i-layer initial growth leads to an increased crystallinity and reduced structural evolution of the i-layer microstructure, which we believe contribute to improved tandem solar cell performance.

4. Conclusions

The effects of microcrystalline silicon i-layer modification near the p/i interface, in a tandem solar cell configuration, have been examined with Raman spectroscopy at different stages of i-layer growth. The results indicate that an improved bottom cell and tandem cell performance can be achieved by a simple two-step process of i-layer modification near the p/i interface. This allows homogeneous growth at the crystallinity level of around I_{CRS} = 50% to be maintained. The results suggest the possibility of relaxing the requirements of the p-layer in terms of nucleation, to eliminate the need to re-optimise the p-layer when the recipe is transferred from a single junction to a tandem device. An initial tandem-cell conversion efficiency of 11.3% has been achieved.

Acknowledgements

This work was part financed by the EC through 038885 (SES6), POWERFOIL project. One of the authors (CD) gratefully acknowledges ATHLET project (No. 019670) for financial assistance.

References

[1] L. Houben, M. Luysberg, P. Hapke, R. Carius, F. Finger, H.Wagner, Philos. Mag. A 77 (1998) 1447.
[2] M. Tzolov, F. Finger, R. Carius, P. Hapke, J. Appl. Phys. 81 (11) (1997) 7376.
[3] P. Roca i Cabarrocas, N. Layadi, T. Heitz, B. Drévillon, I. Solomon, Appl. Phys. Lett. 66 (1995) 3609.
[4] J. Koh, A.S. Ferlauto, P.I. Rovira, C.R. Wronski, R.W. Collins, Appl. Phys. Lett. 75 (15) (1999) 2286.
[5] O. Vetterl, M. Hülsbeck, J. Wolff, R. Carius, F. Finger, Thin Solid Films 427 (46) (2003).
[6] J. Kocka, A. Fejfar, H. Stuchlikova, J. Stuchlik, P. Fojtik, T. Mates, B. Rezek, K. Luterova, V. Svrcek, I. Pelant, Sol. Energy Mater. Sol. Cells 78 (2003) 493.
[7] T. Fujibayashi, M. Kondo, J. Appl. Phys. 99 (2006) 043703.
[8] O. Vetterl, F. Finger, R. Carius, P. Hapke, L. Houben, O. Kluth, A. Lambertz, A. Mück, B. Rech, H.Wagner, Sol. Energy Mater. Sol. Cells 62 (2000) 97.
[9] Y. Mai, S. Klein, X. Geng, M. Hülsbeck, R. Carius, F. Finger, Thin Solid Films 501 (2006) 272.
[10] B. Yan, G. Yue, J. Yang, S. Guha, G.L. Williamson, D. Han, C.-S. Jiang, Appl. Phys. Lett. 85 (11) (2004) 1955.
[11] C. Ross, Y. Mai, R. Carius, F. Finger, MRS Symp. Proc. 862 (2005) A10.4.1.
[12] Y. Mai, S. Klein, R. Carius, J. Wilff, A. Lambertz, F. Finger, X. Geng, J. Appl. Phys. 97 (2005) 114913.
[13] F. Finger, Y. Mai, S. Klein, R. Carius, Thin Solid Films 516 (2008) 728.